

Proton-Induced Plasticity in Hydrogen Clusters

I. Štich,¹ D. Marx,² M. Parrinello,² and K. Terakura^{3,4}

¹JRCAT, Angstrom Technology Partnership, 1-1-4 Higashi, Tsukuba, Ibaraki 305, Japan

²Max-Planck-Institut für Festkörperforschung, Heisenbergstrasse 1, 70569 Stuttgart, Germany

³NAIR, Angstrom Technology Partnership, 1-1-4 Higashi, Tsukuba, Ibaraki 305, Japan

⁴CREST, Japan Science and Technology Corporation (JST), Kawaguchi, Saitama 332, Japan

(Received 23 December 1996)

The effect of protonation of pure hydrogen clusters is investigated at low temperature using a combination of path-integral simulations and first-principles electronic structure calculations. The added proton gets trapped as a very localized H_3^+ impurity in the cluster core, and is surrounded by stable shells of solvating H_2 molecules. These clusters are frozen with respect to the translational degrees of freedom, while the H_2 ligands undergo large-amplitude rotations. The classical approximation for the nuclei fails to account for this effect which is akin to plastic behavior in crystals. [S0031-9007(97)03136-0]

PACS numbers: 36.40.Wa, 67.20.+k, 67.90.+z

Protonated hydrogen clusters represent a unique class of systems in that they consist of a quantum solute in a quantum solvent. Neutral $(\text{H}_2)_n$ and $(\text{D}_2)_n$ (isotropic $J = 0$) clusters, their mixtures including simple impurities, and the related helium clusters are already extensively studied theoretically taking properly into account their quantum character at low temperatures [1]. Let us review a few aspects that set the stage for the present investigation. It was shown that small $(\text{H}_2)_n$ clusters ($n \leq 20$) exhibit extreme quantum behavior and remain quantum-liquid-like down to the ground state, whereas the corresponding deuterium clusters clearly freeze into solidlike structures [1–3]. Other exciting phenomena [1] range from the quantum analog of binary phase separations in isotopically mixed H_2/D_2 clusters [4] to the absence of magic numbers and superfluid behavior [5] similar to that observed in $^4\text{He}_n$ microclusters [6]. By seeding the hydrogen quantum clusters with Li, Hg, or Mg metal atoms a complex impurity-dependent behavior has been found, which leads at times to localization or to liquidlike structures [7,8]. Similarly complex scenarios are known from $^4\text{He}_n$ clusters with impurities [1,9,10].

In light of these findings one can only speculate what precisely happens if a proton is added to a neutral $(\text{H}_2)_n$ microcluster. Does the cluster remain quantum-liquid-like; does the impurity get trapped or does it delocalize; does the proton chemically react; etc.? The experimental quest to answer such questions has a long history [11–17], and the picture that emerged over the years is that of a tightly bound central H_3^+ core which is solvated by shells of H_2 molecules $\text{H}_3^+ \cdot (\text{H}_2)_n$ with “magic numbers” such as $n = 3$ and $n = 3 + 3$ indicating successive shell closures, but see Ref. [18] for a different finding. In particular, infrared predissociation spectroscopy is consistent with a $\text{H}_3^+ \cdot (\text{H}_2)_3$ structure that can be described as three H_2 molecules being attached at the corners of a central H_3^+ triangle [15]. All these assignments, however, are based on quite indirect pieces of evidence possibly to-

gether with underlying models, and structural as well as dynamical details still remain elusive. As an example we mention that, surprisingly, the rotational structure of the observed vibrational bands could not be resolved despite ruled out instrumental artifacts of the sophisticated high-resolution technique [15].

Quantum chemical calculations focused on exploring the potential energy surfaces of small H_n^+ clusters. Such studies [19–22] uncovered that the typical minimum energy structures exhibit a cluster formed by a three-center-bonded H_3^+ moiety with bond lengths in the range of 0.8–0.9 Å, solvated by essentially unperturbed H_2 molecules at distances of typically 1.5 Å in the first shell. It was also stressed that the potential energy surfaces are very flat and anharmonic. Under these circumstances quantum effects are expected to be significant, and it is far from clear whether at low temperatures the structure is dominated by the minimum on the potential energy surface, or if the behavior is more quantum-liquid-like as for the unprotonated $(\text{H}_2)_n$ clusters. The present paper addresses and answers these questions.

To this end we have performed an extensive quantum simulation study of isolated H_n^+ clusters at 5 K in a wide range of sizes, $n = 3, 5, 7, 9$, and 27. We followed the idea of a method [23] that combines path-integral simulations [24] of the nuclei with first-principles electronic structure calculations [25] to describe their interactions in the Born-Oppenheimer approximation. The crucial point is that this technique allows us to explore simultaneously quantum and thermal fluctuations in cases where simple model potentials fail [26], as required here. The electronic structure and the resulting forces on the protons were calculated within Kohn-Sham density functional theory [25] using a generalized gradient approximation [27]. The hydrogen cores were described by a von Barth-Car type norm-conserving pseudopotential [28], and the orbitals were expanded in plane waves with an energy cutoff of 30 Ry in a cubic supercell with an edge length of 30 a.u.;

the positive charge was compensated by a uniform background. The canonical path integral was mapped onto $P = 32$ cyclically connected replicas defining the imaginary time axis [24]. Nuclear exchange was neglected because of the vanishing effect of the Bose-Einstein statistics in the case of $(\text{H}_2)_n$ clusters at 5 K [3], which implies that no nuclear spin symmetry restrictions on the rotational J levels are imposed. The sampling efficiency was increased by using the staging action together with Nosé-Hoover thermostat chains of length 4 coupled separately to each nuclear degree of freedom [29]. A time step of 0.6 fs was used and the fictitious bead mass was set to the physical proton mass. Statistical averages were obtained from about 5×10^3 configurations after equilibration. In addition, we performed simulations with classical protons of the same length.

We checked the accuracy of our electronic structure modeling by comparing the optimized structures with those of correlated configuration interaction with single and double substitutions (CISD) calculations [21] performed for $n \leq 13$. The structures agree within 5% on average with deviations that decay to less than 3% for the largest clusters that we could compare. These static structures are depicted in Fig. 1 and show the expected shell structure around a central H_3^+ core.

The finite-temperature distribution functions of the distances that involve at least one proton of the H_3^+ core are displayed in Fig. 2 for the three largest clusters. The classical simulations at 5 K reveal a pronounced radial structuring corresponding to successive sharp solvation shells that are clearly separated. The peak around 1 Å is split in the case of the H_7^+ cluster in (a), which indicates that the H_3^+ core is asymmetric with two short and one long H-H bond as a result of one and two attached H_2 ligands, respectively. The more symmetric H_9^+ and H_{27}^+ clusters, on the other hand, have a unimodal first peak and thus an equilateral-triangular H_3^+ core. The general picture that emerges from these classical simulations at 5 K is that all the investigated clusters are extremely rigid objects. This character changes if quantum fluctuations are properly taken into account at 5 K. All peaks broaden substantially, in particular, those of the solvation shells, and are not as clearly separated as in the classical approximation. The broadening is particularly severe for our largest cluster, H_{27}^+ , that displays only a broad band after the second minimum. We also simulated the H_7^+ cluster classically at higher temperatures and observed a similar smearing only around 500 K. However, the cluster was unstable and dissociated after about 800 steps into H_5^+ and H_2 fragments, which underlines that quantum effects cannot be mimicked simply by thermal fluctuations. Note that the peak positions in Fig. 2 shift by only around 5% after the inclusion of quantum effects; i.e., the bond distances are essentially unaffected.

At this stage it is interesting to contrast the characteristics of the protonated hydrogen cluster $\text{H}^+ \cdot (\text{H}_2)_{13}$ to its neutral counterpart $(\text{H}_2)_{13}$, which was the subject of path-

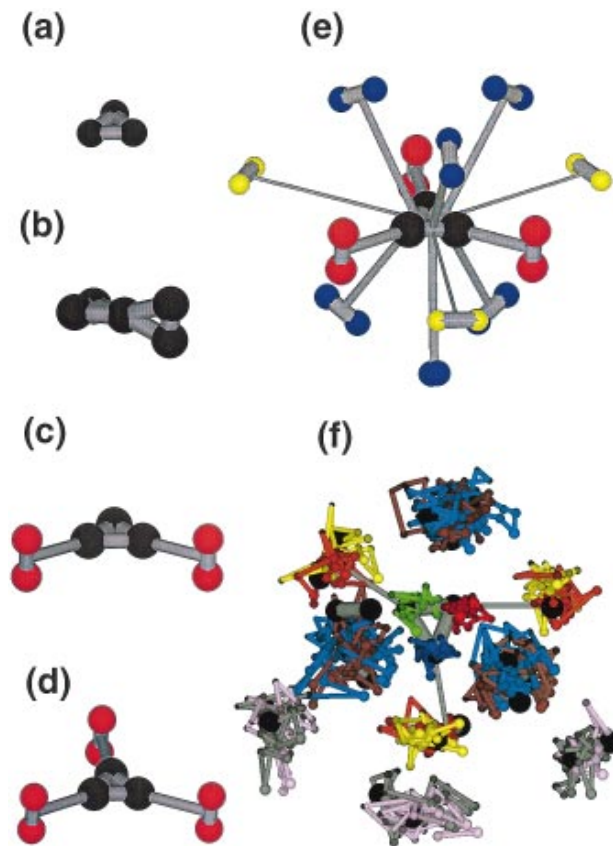


FIG. 1(color). Optimized geometries (point group symmetry) of the protonated hydrogen clusters. (a) H_3^+ (D_{3h}); (b) H_5^+ (C_{2v}); (c) H_7^+ (C_{2v}); (d) H_9^+ (D_{3h}); (e) H_{27}^+ (D_{3h}); (f) snapshot of a full imaginary time path for H_{27}^+ at 5 K. To guide the eye atoms marking the origin of the path are shown by large balls with bonds shown by sticks. Beads in the H_3^+ core ion and in the successive shells are shown in different colors.

integral simulations using a model potential [3]. In order to quantify the floppiness of the cluster these authors computed Lindemann's relative rms bond length fluctuations $\delta = (32.0 \pm 2.0)\%$ and the cluster radius of gyration $R_g = 4.5 \pm 0.2$ Å based on the molecular centroid distances at 5 K; see Ref. [2] for similar quantum ground-state results. The numbers are in remarkable contrast with what we calculate in the protonated case, namely, $\delta \approx (2 \times 10^{-7})\%$ and $R_g \approx 2.7$ Å. The dramatic reduction of δ by many orders of magnitude signals a proton-induced freezing out of the internal translational molecular degrees of freedom; note that clusters are commonly considered as liquidlike if δ exceeds about 10%. Furthermore, the reduction by a factor of 2 of the cluster size R_g reflects a strong electrostrictive effect which is responsible for these phenomena. Similar numbers have been obtained for H_7^+ and H_9^+ , which strongly suggests that these are generic features.

Given this rigidity, one might ask the reason for the substantial broadening observed in Fig. 2. The answer can be found in Fig. 3 which shows in (a) that the H_2 ligands can undergo very large-amplitude rotations.

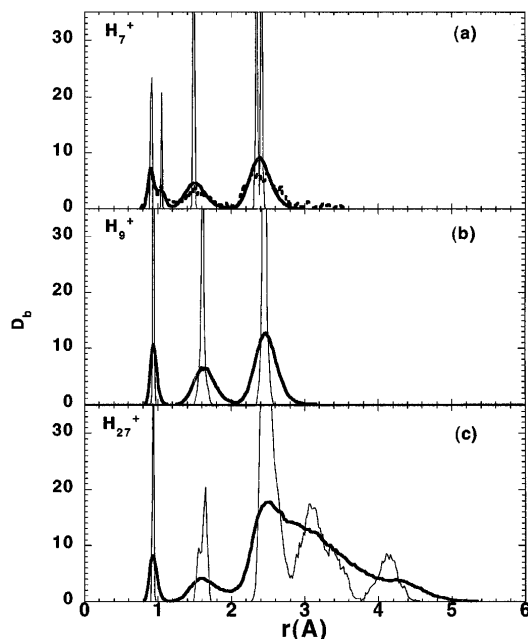


FIG. 2. Normalized partial distribution functions $[\int D_b(r) dr = n - 1]$ of bond distances involving at least one proton from the H_3^+ core. (a) H_7^+ , (b) H_9^+ , and (c) H_{27}^+ . Bold solid lines: quantum simulation at 5 K; light solid lines: classical simulation at 5 K; dashed line in (a): classical simulation of H_7^+ at 500 K (this particular trajectory contains only about 800 configurations because the cluster dissociated into H_5^+ and H_2).

These rotations are much reduced in the classical case (b) and hence are a quantum-induced phenomenon. The combination of a rigid translational structure together with the pronounced rotational softness can be referred to as “quantum plasticity.”

The degree to which the different protons behave like quantum mechanical particles can be put on a quantitative footing in terms of the rms position displacement correlation function $\mathcal{R}_I(\Delta\tau) = \langle |\mathbf{R}_I(\tau) - \mathbf{R}_I(\tau')|^2 \rangle^{1/2}$ where $0 \leq \Delta\tau = \tau - \tau' \leq \beta\hbar$ with $\beta = 1/k_B T$ and $\mathbf{R}_I(\tau)$ denotes the coordinate of particle I at imaginary time τ . The midpoint value $\mathcal{R}_I(\beta\hbar/2)$ of this function is a measure of the particle’s spatial “size,” whereas its variation in imaginary time determines the degree of ground-state dominance and thus localization [30]. Localized states with a large energy gap ΔE between ground and excited states are characterized by a constant function in the range of roughly $\hbar/\Delta E < \Delta\tau < \beta\hbar - \hbar/\Delta E$, whereas $\mathcal{R}_I(\Delta\tau)$ varies over the entire $\Delta\tau$ range for extended quantum states.

These correlation functions are depicted in Fig. 4(a) for the three core protons that constitute the H_3^+ unit for all clusters studied. First of all, one observes a clear trend of decreasing size of the three protons as the cluster grows: the $\mathcal{R}(\beta\hbar/2)$ extension of the protons shrinks by a factor of more than 2 from the bare H_3^+ ion to the core of H_{27}^+ . More importantly, it turns out that these protons seem to be tightly localized in the H_9^+ , and even more so in the H_{27}^+ clusters as proven by the flat

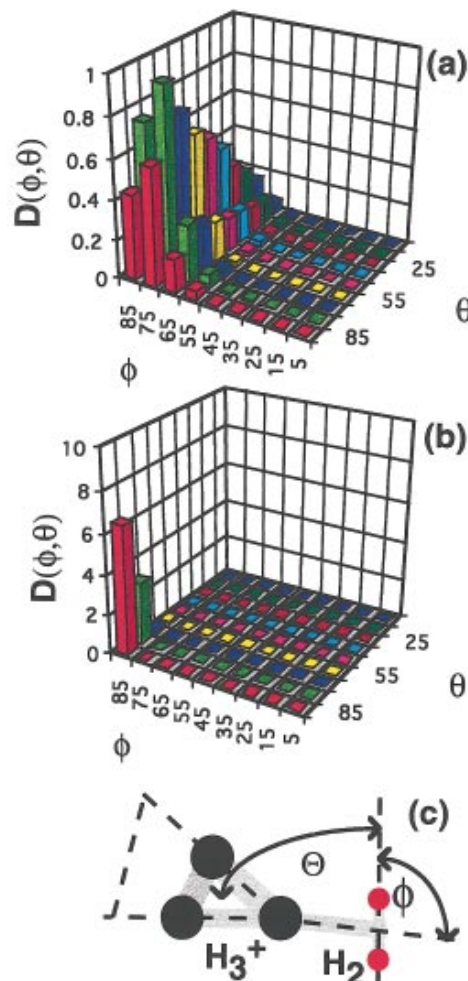


FIG. 3(color). Angular distribution $D(\Theta, \Phi)$ of the first-shell H_2 molecules relative to the H_3^+ core ion for H_9^+ at 5 K. Θ is the angle between the H_3^+ plane and the H-H axis of the H_2 molecule, and Φ the angle between the H-H axis and the connection between its center of mass and the closest proton of the H_3^+ core; both angles are taken to be the smallest angles of twist. The distributions are normalized to an arbitrary constant. (a) Quantum simulation, (b) classical simulation, and (c) definition of angles Θ and Φ .

correlation functions for $\Delta\tau$ larger than about $0.2\beta\hbar$. We thus conclude that the closure of the first solvation shell at H_9^+ induces a pronounced ground-state dominance and localization on the H_3^+ core ion, a trend that is enforced in the larger H_{27}^+ cluster with a second solvation shell and an onset of a third one. The localization properties in successive solvation shells are analyzed separately in Fig. 4(b) for the largest cluster. Here, it becomes evident that the H_3^+ core protons of H_{27}^+ are clearly ground-state dominated, whereas those of the solvating H_2 ligands are much more delocalized in space, which goes hand in hand with the rotational delocalization of the ligands. Furthermore, there is a clear trend that the H_2 delocalization increases systematically from inner to outer solvation shells. This behavior is shown pictorially in Fig. 1(f) showing a typical snapshot of the distribution of beads representing the proton density.

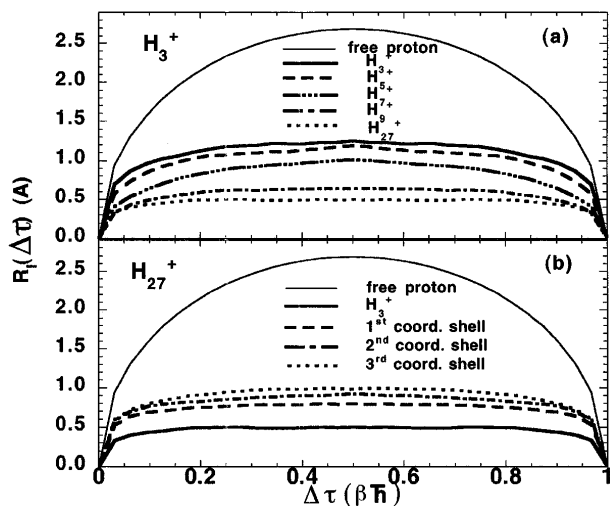


FIG. 4. Root-mean-square position displacement functions in imaginary time $\mathcal{R}_r(\Delta\tau)$ at 5 K. (a) H_3^+ core protons in H_n^+ for $n = 3, 5, 7, 9,$ and 27 ; (b) protons in the H_3^+ core and in the successive solvation shells in H_{27}^+ . For reference the free proton function is shown in light lines.

In conclusion, we demonstrated that protonation of pure hydrogen clusters has a dramatic effect on bonding, structure, and properties of these clusters. The added proton induces “translational freezing” of the quantum-liquid-like neutral clusters and imposes a clear solvation shell structure around a centrally trapped and tightly localized H_3^+ impurity core. In spite of this, a classical description of the nuclei artificially overemphasizes the rigidity. In particular, we uncovered that the quantum fluctuations affect mostly the rotations of the solvating hydrogen molecules and cause “quantum plasticity.” Thus, it is tempting to speculate that the failure to resolve spectroscopically the rotational structure [15] might be a consequence of this plasticity. This behavior should be contrasted to that of a proton in aqueous environments [31]. Here the proton attaches to a H_2O molecule to form H_3O^+ as the smallest chemical unit. Contrary to the inert and actually stabilizing H_3^+ core, the former complex makes proton migration possible via dynamical making and breaking of various complexes such as H_5O_2^+ and H_9O_4^+ . In this respect protonated hydrogen clusters behave similar to CH_5^+ solvated by H_2 molecules [32]. Successive solvation shells are found to be more mobile in both cases and the core ion, i.e., CH_5^+ and H_3^+ , is the more localized and rigid the more H_2 ligands are attached to it.

The calculations were performed on the JRCAT supercomputer system. This work was partly supported by New Energy and Industrial Technology Development Organization (NEDO).

[1] K. B. Whaley, *Int. Rev. Phys. Chem.* **13**, 41 (1994); R. N. Barnett and K. B. Whaley, *Z. Phys. D* **31**, 75 (1994).

- [2] M. V. Rama Krishna and K. B. Whaley, *Z. Phys. D* **20**, 223 (1991); M. A. McMahon and K. B. Whaley, *Chem. Phys.* **182**, 119 (1994).
- [3] D. Scharf, G. J. Martyna, and M. L. Klein, *Chem. Phys. Lett.* **197**, 231 (1992); *J. Chem. Phys.* **97**, 3590 (1992).
- [4] C. Chakravarty, *Phys. Rev. Lett.* **75**, 1727 (1995).
- [5] P. Sindzingre, D. M. Ceperley, and M. L. Klein, *Phys. Rev. Lett.* **67**, 1871 (1991).
- [6] P. Sindzingre, M. L. Klein, and D. M. Ceperley, *Phys. Rev. Lett.* **63**, 1601 (1989).
- [7] D. Scharf, G. J. Martyna, and M. L. Klein, *J. Chem. Phys.* **99**, 8997 (1993).
- [8] S. Broude and R. B. Gerber, *Chem. Phys. Lett.* **258**, 416 (1996).
- [9] S. Goyal, D. L. Schutt, and G. Scoles, *Phys. Rev. Lett.* **69**, 933 (1992).
- [10] Y. Kwon, D. M. Ceperley, and K. B. Whaley, *J. Chem. Phys.* **104**, 2341 (1996).
- [11] R. Clampitt and L. Gowland, *Nature (London)* **223**, 815 (1969).
- [12] K. Kiraoka and P. Kebarle, *J. Chem. Phys.* **62**, 2267 (1975); K. Hiraoka, *J. Chem. Phys.* **87**, 4048 (1987); K. Hiraoka and T. Mori, *Chem. Phys. Lett.* **157**, 467 (1989).
- [13] A. van Lumig and J. Reuss, *Int. J. Mass Spectrom. Ion Phys.* **27**, 197 (1978).
- [14] D. Mathur and J. B. Hasted, *Nature (London)* **280**, 573 (1979).
- [15] M. Okumura, L. I. Yeh, and Y. T. Lee, *J. Chem. Phys.* **88**, 79 (1988); *J. Chem. Phys.* **83**, 3705 (1985).
- [16] Y. K. Bac, P. C. Cosby, and D. C. Lorents, *Chem. Phys. Lett.* **159**, 214 (1989).
- [17] W. Paul *et al.*, *Int. J. Mass Spectrom. Ion Process.* **149/150**, 373 (1995); *Chem. Phys.* **209**, 265 (1996).
- [18] S. Ouaskit *et al.*, *Phys. Rev. A* **49**, 1484 (1994).
- [19] S. W. Harrison, L. J. Massa, and P. Solomon, *Nature (London) Phys. Sci.* **245**, 31 (1973).
- [20] Y. Yamaguchi, J. F. Gaw, and H. F. Schaefer III, *J. Chem. Phys.* **78**, 4074 (1983).
- [21] M. Farizon *et al.*, *Chem. Phys. Lett.* **177**, 451 (1991); M. Farizon, H. Chermette, and B. Farizon-Mazuy, *J. Chem. Phys.* **96**, 1325 (1992).
- [22] T. Pang, *Chem. Phys. Lett.* **228**, 555 (1994).
- [23] D. Marx and M. Parrinello, *Z. Phys. B* **95**, 143 (1994); *J. Chem. Phys.* **104**, 4077 (1996).
- [24] D. M. Ceperley, *Rev. Mod. Phys.* **67**, 279 (1995).
- [25] M. C. Payne, M. P. Teter, D. C. Allan, T. A. Arias, and J. D. Joannopoulos, *Rev. Mod. Phys.* **64**, 1045 (1992).
- [26] D. Marx and M. Parrinello, *Nature (London)* **375**, 216 (1995); *Science* **271**, 179 (1996).
- [27] J. P. Perdew *et al.*, *Phys. Rev. B* **46**, 6671 (1992).
- [28] P. Giannozzi (private communication).
- [29] M. E. Tuckerman, D. Marx, M. L. Klein, and M. Parrinello, *J. Chem. Phys.* **104**, 5579 (1996).
- [30] D. Chandler and K. Leung, *Annu. Rev. Phys. Chem.* **45**, 557 (1994).
- [31] M. Tuckerman, K. Laasonen, M. Sprik, and M. Parrinello, *J. Chem. Phys.* **103**, 150 (1995).
- [32] D. W. Boo *et al.*, *Science* **269**, 57 (1995); D. W. Boo and Y. T. Lee, *J. Chem. Phys.* **103**, 520 (1995).